Journal of The Electrochemical Society, **162** (7) D275-D282 (2015)
0013-4651/2015/162(7)/D275/8/$33.00 © The Electrochemical Society

Electrochemical Characterization of a Cu(II)-Glutamate Alkaline Solution for Copper Electrodeposition

P. Pary,[a,b,z] L. N. Bengoa,[a,b] and W. A. Egli[a]

[a]*Center for Paints and Coatings Development (CICBA-CONICET), La Plata B1900AYB, Argentina*
[b]*Engineering School, National University of La Plata, La Plata B1900AYB, Argentina*

In this study, a cyanide-free electrolyte containing glutamate as a complexing agent is investigated as a more environmentally friendly alternative for alkaline copper plating. The solution was prepared using copper sulfate, sodium glutamate and potassium hydroxide. The pH of the electrolyte (pH = 8) and the ratio ligand:copper (R = 3), were chosen from equilibrium diagrams in order to avoid the formation of insoluble complexes and oxides. The electrochemical response of the system was determined by means of cyclic voltammetry. The results showed that copper electroreduction occurs in a two steps pathway with a cuprous-glutamate complex as an intermediate. Galvanostatic deposits obtained from the bath under study had proper brightness and roughness at the selected current density conditions. Scanning electron microscopy and X-Ray diffraction were carried out in order to characterize deposits surface morphology and crystal orientation. Chronoamperometric experiments together with atomic force microscopy proved that copper deposits grow through an instantaneous nucleation mechanism in which nuclei are not exactly spherical. These preliminary studies suggest that the Cu^{+2}-glutamate electrolyte may be suitable for the replacement of cyanide baths in copper electrodeposition at high pH without the need of additives as this electrolyte acts as a self-levelling system. Also, the use of this electrolyte could eliminate the need of performing strike deposits on less noble substrates, allowing a one step plating process.

Manuscript submitted March 9, 2015; revised manuscript received April 10, 2015. Published April 18, 2015.

Cyanide based electrolytes have been used in the electroplating industry for several years to obtain good quality copper, zinc, silver and gold metallic coatings. However, due to their high toxicity and extremely negative impact on the environment during waste disposal,[1] these electrolytes are currently being replaced with cyanide-free plating baths. For the case of zinc, these are mainly strong alkaline solutions where the complexing and polarizing functions of cyanide are performed by negatively charged metallic anions in conjunction with some organic additives. The latter are potentially suitable for the production of zinc deposits according to the industrial quality requirements and, thus, have become an important subject of study.

Likewise, copper electrodeposition has been carried out using alkaline cyanide-containing electrolytes to produce thin coatings that serve as a protective layer for subsequent plating processes (strike coatings) on substrates less noble than copper. For example, automotive parts industry applies this technique on pieces manufactured with zamak, a zinc-aluminum alloy, which also contains copper, magnesium and lower concentrations of iron, nickel, lead and cadmium.[2] Since this alloy, as well as zinc and steel substrates, cannot be copper-plated directly from acid sulfate electrolytes due to copper cementation reaction and lack of adherence, a copper undercoat deposited from alkaline baths where the substrate is passive, is essential to achieve the pursued objective.[3,4] As mentioned before, the high toxicity of the cyanide group together with the implementation of more severe environmental regulations have directed researchers' efforts toward the search of new, more friendly to the environment and less toxic alternatives.

Many formulations have been studied so far,[5–13] all of which contain a compound that acts as a complexing agent preventing copper oxide precipitation at pH values higher than 4. For example, it is known that amino acids have the ability to react with copper leading to the formation of stable complexes.[14] Among these, amino acids having a second carboxylic group, such as aspartic and glutamic acids, have proved to be much more effective as addition agents than those containing only one carboxylic group, of which glutamic acid ($C_5H_{10}NO_4$) has the strongest effect.[15] Furthermore, this compound forms negatively charged complexes with Cu^{+2} at pH values higher than 4 as cyanide does with Cu^{+}. Based on this, it could be expected that glutamate anion (Glu^{-2}) would be a good substitute for cyanide, instead of being just an additive, in systems where alkaline conditions are necessary.

The aim of the present work is to study the Cu^{+2}-glutamate system and evaluate its suitability for mild alkaline copper plating (pH = 8). To that end, cyclic voltammetry (CV) and chronoamperometry were chosen as the main electrochemical techniques to study this new copper plating electrolyte, while scanning electron microscopy (SEM), X-rays diffraction (XRD), atomic force microscopy (AFM), mirror reflectance (MR) evaluation and internal stresses measurement were used to characterize the deposits obtained.

[z]E-mail: anelpire8@cidepint.gov.ar

Experimental

The electrolyte used throughout this work was a 0.20 mol l^{-1} Cu^{+2} and 0.60 mol l^{-1} glutamate solution prepared by dissolving $CuSO_4.5H_2O$ (Cicarelli rg) and $C_5H_8NNa0_4$ (Anedra rg) in distilled water. The pH was adjusted to eight by addition of KOH (Anedra 99%).

A standard three-electrode cell with a platinum rotating disc electrode (0.04 cm^2) as working electrode was used, using a copper wire (4.70 cm^2) as counter electrode and a saturated calomel electrode (SCE) as reference electrode. All the electrochemical potential values in this work are expressed in this scale. Temperature was held at 60°C using a FRIGOMIX 1495 thermostat. This temperature was selected from previous stationary and rotating Hull cell tests performed with this plating bath (to be published).

Equilibrium diagrams for the copper-glutamate system were built using the MEDUSA software developed by the Royal Institute of technology (KTH) of Stockholm, Sweden.[16] All the chemical equilibrium constants and the electrochemical potential equilibria were taken from literature.[14,17]

The Ohmic drop was negligible due to the high conductivity of the electrolyte ($\kappa \approx 150\ S \cdot cm^{-1}$), which was taken from electrochemical impedance data. The uncompensated resistance was estimated[18] and the results showed that the ohmic drop reaches a maximum value of 4 mV at the highest current density (CD) registered. Migration effects cannot be ignored in the present work, and therefore, quantitative data analysis was not possible.

CV was carried out using an EG&G Princeton Applied Research potenciostat-galvanostat model 273A connected to a computer and controlled with Corrware2 software. The potential was swept between −1.0 V and 1.0 V at different scan rates (v, $V \cdot s^{-1}$) with and without rotation of the working electrode. In addition, the cathodic switching potential (SP) was varied. Galvanostatic deposits, 15 μm thick, were obtained at different CDs on bright steel (Ra < 0.5 μm) substrates (Q-Panel Smooth Finish QD-36, 0.50 mm × 20 mm × 20 mm) previously pickled in a 10 vol% sulfuric acid solution. The resulting deposits were washed with distilled water and ethanol and then fast-dried with a warm air jet. The steel substrates were weighed

before and after deposition experiments and cathodic current efficiency (CE) was calculated according to Faraday's law. These deposits were characterized by XRD using a Philips 3020 goniometer and a PW 3710 controller with CuKα radiation (λ = 1.54 Å) and a nickel filter. The detector was swept between 10° and 100° with a 0.04° step and 2 seconds per step. The texture and preferred orientation of the copper deposits were determined using the relative texture coefficient (RTC), which was calculated using Eq. 1.

$$RTC\ (\%) = \frac{I_{hkl}/I^0_{hkl}}{\sum_{n=1}^{5} I_{hkl}/I^0_{hkl}} \times 100 \qquad [1]$$

where I_{hkl} and I^0_{hkl} are the diffraction intensities of the crystal plane (hkl) in the sample and a standard Cu powder sample with random orientation repectively.

Potentiostatic deposition was carried out for short times in order to clarify the copper nucleation mechanism on the Q-Panel QD-36 steel substrates. Potentials were chosen from the previously recorded CV's to evaluate its effect on copper nuclei growth. For size and nuclei density estimation, these samples were analyzed using AFM.

All deposits obtained were characterized by SEM using a Quanta200 FEI microscope (Tungsten filament source) equipped with an EDS detector. MR of theses coatings was determined by means of a Datacolor 600 dual-beam d/8° spectrophotometer (Pulse Xenon radiation).

Internal stress measurements were carried out using the bent strip technique with a Specialty Testing & Development Co. plating cell and nickel-iron alloy test strips (PN:2042B). CD was varied and deposition time was set to obtain a deposit thickness (t) of 2.54 μm according to the recommendations given in the standard procedure. Afterwards, the test strips were washed with distilled water, ethanol and fast-dried with a warm air jet. The total number of spread increments of the strip legs (U) was measured with PN 683 deposit stress analyzer. Finally, internal stress (S), in kPa, was calculated using Eq. 2:

$$S = \frac{UKM}{3t} \qquad [2]$$

where M is the ratio between the elasticity modulus of the deposit and that of the substrate (1.43) and K is the calibration constant of the substrate (39.94 Nm^{-1}).

Results and Discussion

Equilibrium diagrams.— The alkalinity of the electrolyte was selected at pH = 8 to avoid the formation of neutral and/or protonated species such as CuGlu, $CuGlu_2H^-$, $CuGlu_2H_2$, $CuGluH^+$, $CuGluH_2^{+2}$, formed at lower pH values,[19] and also to hinder the formation of cuprate anions like $Cu(OH)_3^-$ at higher values.[17] Equilibrium diagrams were built for different Glu^{-2}/Cu^{+2} ratios (R) at the chosen pH value. According to these equilibria calculations, at higher R the stability of the cuprous oxide ($Cu_2O_{(s)}$) decreases, and it disappears from the system when R ≥ 3. This is consistent with the results reported by Liang and Olin[20] for Cu^{+2}-Aspartate complexes and by Survila and Uksiené[5] for Cu^{+2}-Glycine, which showed that the presence of α and β aminoacids as coordination ligands suppresses $Cu_2O_{(s)}$ formation and stabilizes soluble cupric species at pH > 6. As can be seen in Figs. 1 and 2, for the electrolyte under study at R = 3 and pH = 8, the only soluble species present is $CuGlu_2^{-2}$. This is in complete agreement with the results reported by other authors.[9,19,21] Consequently, in order to avoid the formation of insoluble complexes and oxides, the values of R = 3 and pH = 8 were selected.

Cyclic voltammetry.— The CVs shown in Fig. 3 were recorded with a platinum cathode for different v under stationary conditions. When electrode potential is swept in the cathodic direction, one peak is detected (Ic) at potentials between −0.84 V to −0.90 V depending on v, after which CD attains a limiting value. Two cathodic peaks are usually found for copper electrodeposition from electrolytes containing ammonia,[22] picolinic acid[23] or histidine.[8] However, only one peak is detected for Cu^{+2} – Glycine complexes[9,24] and for Cu^{+2} in weakly acidic sulfate electrolytes.[25] In the present work, the occurrence of only one cathodic peak can be explained by the similarity with the glycine electrolyte and by the excess of ligand present in the solution.[26] Peak current density (jp) and peak potential (Ep) presented a linear dependency with $v^{1/2}$ and v respectively (not shown), which is characteristic of an irreversible process.[27,28] This behavior is very similar to the one reported by Bolzán for copper electroreduction on glassy carbon electrodes.[23] The cathodic process generally ascribed to I_c is the reduction of cupric ions to metallic copper usually in a consecutive two steps pathway.[22,23,29,30] For the $CuGlu_2^{-2}$ electrolyte

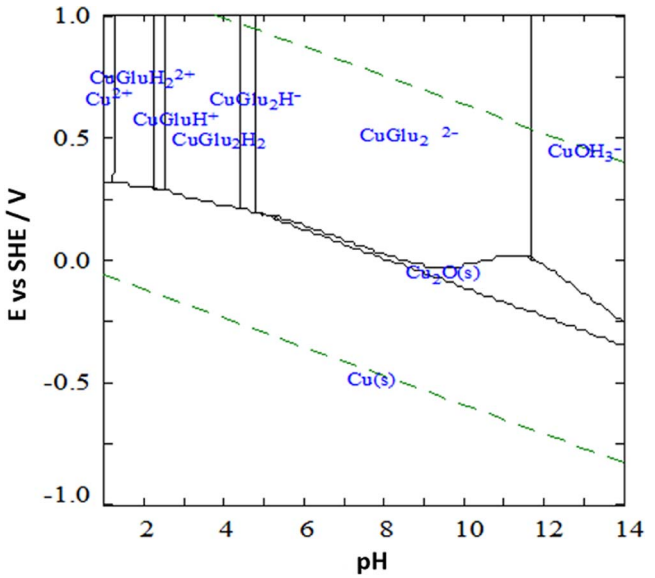

Figure 1. Equilibrium diagram for a Cu^{+2}/glutamate R = 3 at 50°C with $[Cu^{+2}] = 0.20$ mol l^{-1}.

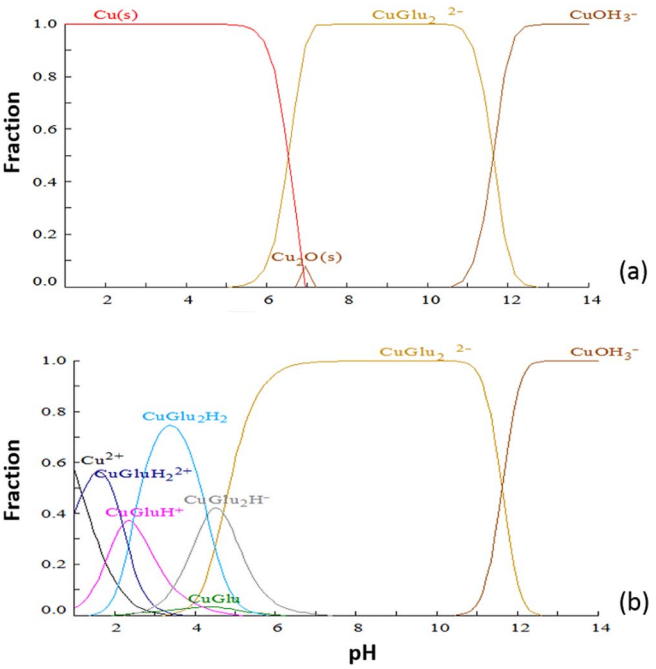

Figure 2. Species distribution as a function of the pH at 50°C with $[Cu^{+2}] = 0.20$ mol l^{-1} for (a) E = 0.17 V/SCE and (b) E = 0.26 V/SCE.

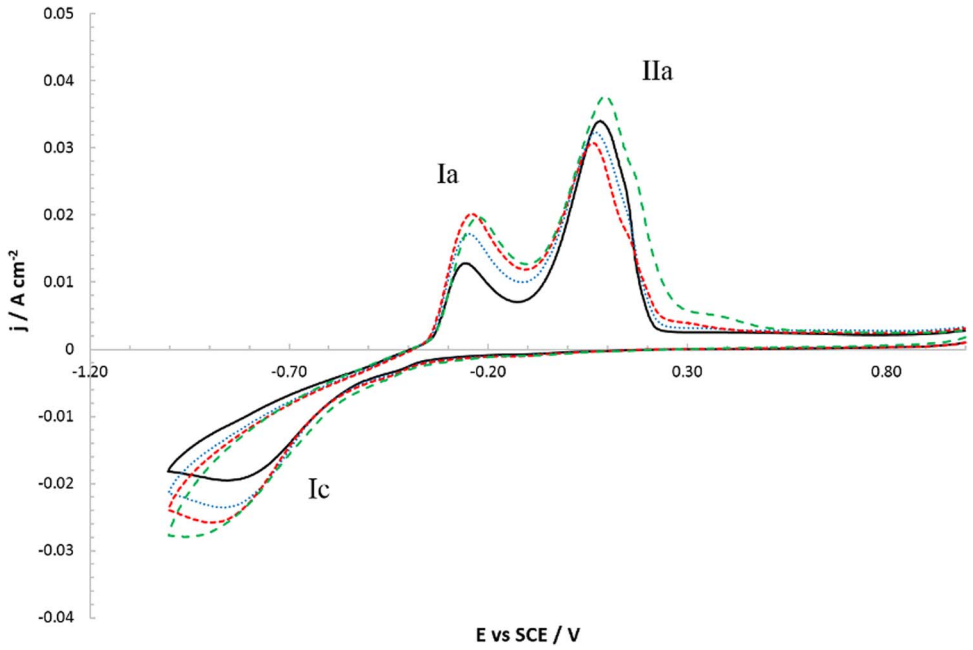

Figure 3. Cyclic voltammograms recorded at 0.02 (—), 0.03 (· · · ·), 0.04 (- - -) and 0.05(– – –) V s^{-1} on a stationary electrode.

the following reactions can be proposed,

$$CuGlu_2^{-2} + e^- \rightarrow Cu^{+*} \quad [3]$$

$$Cu^{+*} + e^- \rightarrow Cu + 2Glu^{-2} \quad [4]$$

where Cu^{+*} stands for some complex formed between Glu^{-2} and Cu^{+}. Based on the few cases reported in the literature for cuprous complexes with organic amines,[31] it is reasonable to assume that the formation constants of Cu^{+}-Glu^{-2} would be very similar to the Cu^{+2}-Glu^{-2} complexes. According to the Bockris-Mattson mechanism, the first electrochemical step is the slower one and Eq. 4 has to occur immediately after Eq. 3 to have only one cathodic peak. Some authors have proposed that the direct reduction of cupric complexes to metallic copper takes place in a two-electron electrochemical reaction.[9,32] If that were the case, the cathodic process in glutamate electrolyte would be represented by the following reaction,

$$CuGlu_2^{-2} + 2e^- \rightarrow Cu + 2Glu_2^{-2} \quad [5]$$

During the reverse anodic scan, after SP = −1.0 V, two anodic peaks appeared, marked as I_a (*Ep* = −0.25 V) and II_a (*Ep* = 0.10 V) in Fig. 3. The absence of a crossover between the direct and the reverse scan in the cathodic potential region of the CVs indicates that 3D nucleation and growth of metallic copper is not the rate-controlling step. Similar behavior was observed previously for Cu^{+2} deposition from a sulfate electrolyte in presence of histidine at pH = 6[8] and in absence of ligands at pH = 3.7.[25]

For I_a, *Ep* was constant while *jp* was a linear function of $v^{1/2}$ (not shown). This fact leads to the conclusion that the process involved in this peak is reversible and under diffusional kinetic control.[27] The electrochemical process taking place at this peak may be related to oxidation of Cu^{+*} species generated by reaction 3 during the cathodic sweep. The increase in peak height observed when *v* is raised supports the first hypothesis as less Cu^{+*} is consumed in the cathodic branch when scanning is performed at higher rates. On the contrary, for peak II_a neither *jp* nor *Ep* were affected significantly by *v*. The latter suggests that this oxidation process is reversible and under activation control. This evidence and the shape of peak II_a, i.e. more symmetric and sharper, indicates that electrochemical dissolution of metallic copper is responsible for it.[25] Despite some obvious differences in *Ep* values, this peak has been ascribed to electrochemical dissolution of metallic copper in a large variety of different electrolyte compositions and substrates.[8,9,22,23,25,30,32–35] Another distinct feature of this peak is the appearance of a small shoulder at more anodic potentials, which becomes more evident as *v* increases. This effect has been usually assigned to the disproportionation reaction due to free Cu^{+2} accumulation near the electrode surface and the subsequent oxidation of the Cu^{+} generated.[22]

Similar CV experiments were carried out rotating the working electrode at 1500 rpm. As can be seen in Fig. 4, I_c disappeared upon rotation of the disc and the forward and backward cathodic scans now coincide, indicating that the cathodic process is under activation control. Peak I_a is also reduced to a very small shoulder due to removal of Cu^{+*} soluble species, generated during the cathodic sweep, from the vicinity of the cathode surface on account of forced convection. This supports the mechanism of reactions 3 and 4. The charge corresponding to I_a is ≈300 $\mu C \cdot cm^{-2}$, which is in agreement with the value of 353 $\mu C \cdot cm^{-2}$ required to form a monolayer of Cu_2O reported by Abrantes, Castillo, Norman & Peter[36] suggesting that it could be the result of the oxidation of a monolayer of Cu^{+*} adsorbed species. Regarding the second anodic peak (II_a), it was observed that an increase in *v* from 0.02 to 0.05 V s^{-1} does not change significantly *jp* nor *Ep* and a slight splitting appears (III_a). Despite some differences among the curves, sweeping rate has little influence on the CVs. To understand the appearance of the additional peak it must be noticed that the renewal of solution caused by electrode rotation avoids free Cu^{+2} accumulation at the cathode. As it has been reported,[33] copper complexes with aminoacids inhibit copper dissolution through disproportionation. Taking into consideration that for III_a, *Ep* ≈ 0.30 V it is also possible that the direct oxidation of metallic copper to cuprous species could play a role through the equilibria,[17]

$$Cu = Cu^+ + e \qquad E_0 = 0.28 + 0.0591 \ \log(Cu^+)$$

Another possible explanation of this effect could be the existence of some inhomogeneity in the adsorption energy of the substrate active sites.[23] Nevertheless, no concrete conclusions can be reached based on these experiments, carried out only to identify the different electrochemical processes involved in the Cu^{+2}-glutamate system. A mechanism description of copper deposition and dissolution is out of the scope of this work.

To better understand the electrochemistry of the $CuGlu_2^{-2}$ electrolyte, the SP in the CV was varied and the results are shown in

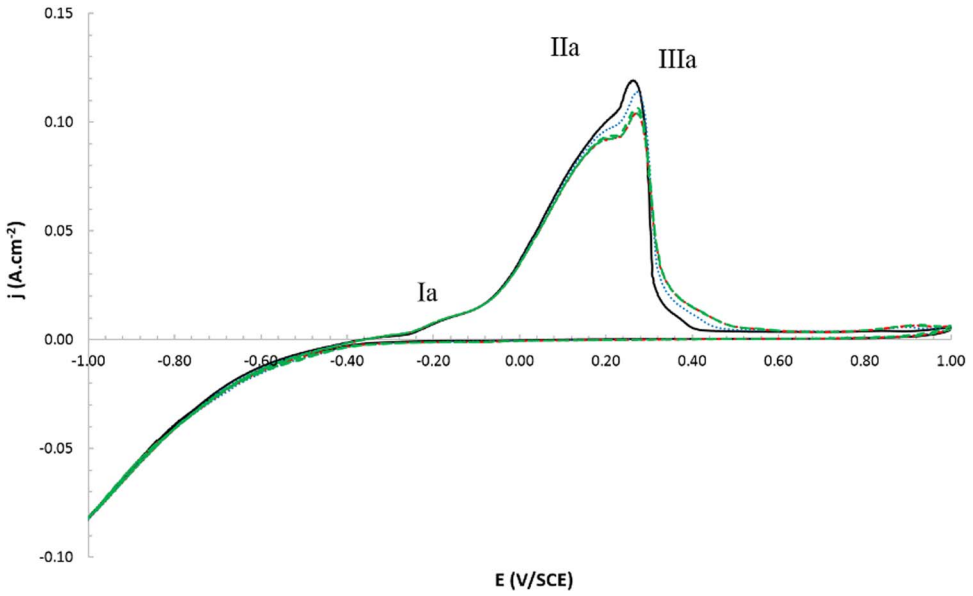

Figure 4. Cyclic voltammograms recorded at 0.02 (—), 0.03 (· · · ·), 0.04 (- - -) and 0.05(– – –) V s^{-1} at 1500 rpm.

Figs. 5 and 6. Two rather different behaviors were observed for the stationary and the rotating electrode. In the first case, there is initially only one small anodic peak at $E = -0.05$ V which splits in two peaks for SP ≤ 0.60 V. The first anodic peak grows linearly with SP, indicating that more Cu^{+*} species are formed at more cathodic SP's. When the electrode was rotated at 1500 rpm, this peak was almost absent and again, as in Fig. 4, only a small shoulder is obtained for all SP's. II_a peak appeared at higher positive values for more cathodic SP, corresponding to a larger amount of bulk copper deposit that is oxidized according to the electrochemical reactions previously discussed.

Galvanostatic copper deposits.— Three galvanostatic copper deposits were obtained on steel electrodes at 0.005, 0.01 and 0.02 A · cm^{-2}. These CD values were chosen to produce bright, semi bright and matte copper deposits based on the previous Hull cell studies mentioned in the Experimental section. Both, bright and matte deposits were smooth and adherent, whereas the semi-bright deposit detached easily from the steel substrate. Fig. 7 shows SEM images at 10000× magnification of the three samples. It was seen that the surface of the bright and semi-bright deposits presented a very smooth, slightly globular morphology (Fig. 7a and 7b), characteristic of an electrodeposition process under mixed activation-diffusion control.[37] In contrast, the images for the third sample showed dendrite precursors growths (Fig. 7c) typical of deposit growth under activation control.[37] It is important to mention that the semi-bright sample presented well defined cracks. For the three CDs studied, CE $\geq$ 99%, leading to the conclusion that the Cu^{+*} species are completely reduced under galvanostatic cathodic conditions.

The internal stresses of the coatings for all the CDs were tensile stresses as each leg of the electrode bent concave on its plated face. Results calculated from Eq. 2 showed an increase in the stress from 210 to 421 kPa when the CD varied from 0.005 A · cm^{-2} to

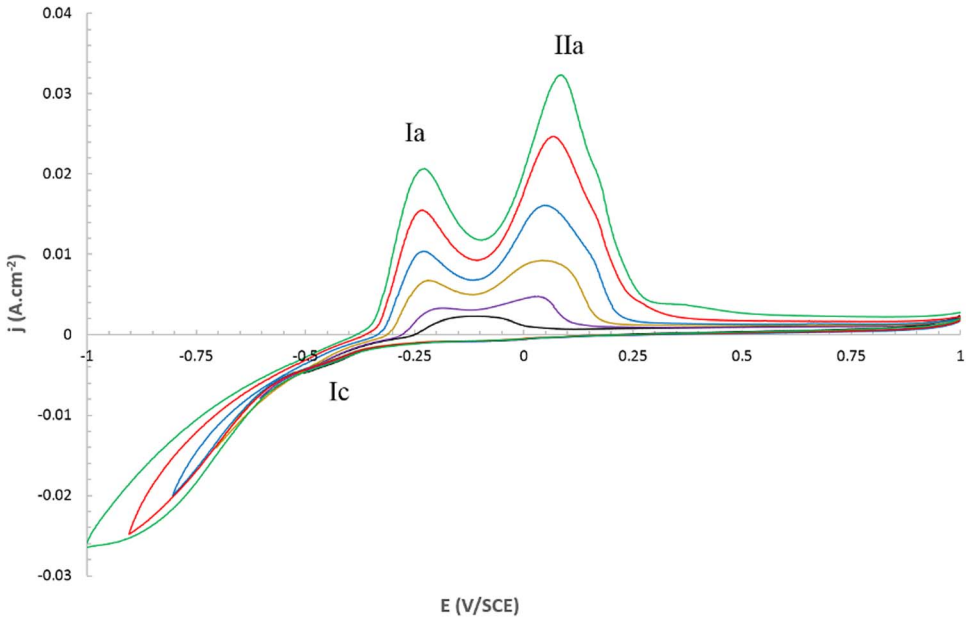

Figure 5. Cyclic voltammograms recorded at 0.05 V s^{-1} on a stationary electrode with variation of the switching potential.

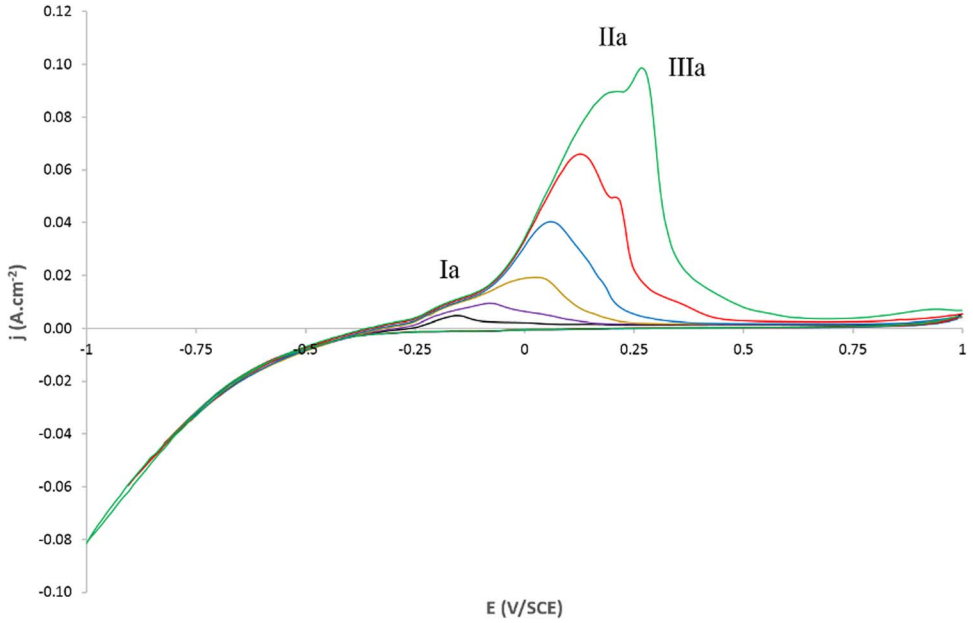

Figure 6. Cyclic voltammograms recorded at 0.05 V s^{-1} rotating the electrode at 1500 rpm with variation of the switching potential.

0.01 A $\cdot$ cm^{-2}. Afterwards, the stress value decreased to 289 kPa for a CD of 0.02 A $\cdot$ cm^{-2}. This result explain the presence of cracks and the loss of adherence in the semi-bright deposit, caused by the considerable increase of the internal tensile stress for the coating obtained with the intermediate CD value.

The MR of the samples as a function of the wavelength can be seen in Fig. 8. It can be seen that for the sample corresponding to CD 0.005 A $\cdot$ cm^{-2}, the reflection is mostly mirror for wavelengths $\geq$ 600 nm. As expected, when CD increases, the degree of mirror reflectance decreases reaching approximately 50% for the 0.01 A $\cdot$ cm^{-2} sample and being less than 30% for the 0.02 A $\cdot$ cm^{-2} deposit. For wavelengths $\leq$ 600 nm, the differences are less relevant.

The XRD spectra are presented in Fig. 9. For the three samples, the RTC (111) was superior to 50% while the RTC for the other four peaks did not exceed 20% (Table I).

The latter indicates that copper deposits are highly orientated with the plane (111) facing the surface of the coating. As this preferred orientation is the same for the three copper deposits, it can be concluded that coating surface morphology is the main factor that defines its brightness, instead of its texture, as reported by Nikolic, Novakovic, Rakocevic, Durovic & Popov[38,39] for copper and zinc deposits.

Potentiostatic deposits.— Potentiostatic deposits were carried out at −0.50 V, −0.60 V and −0.75 V for 2.5 s, in order to analyze the nucleation mechanism for this system. According to literature,[22,30,40] there are two theoretical basic nucleation mechanisms: instantaneous nucleation, in which the nuclei grow on a small number of active sites activated at the same time; and progressive nucleation, where the nuclei grow on a small number of active sites which activate progressively as electroreduction goes on. The models proposed by Scharifker and Hill[40] (Eqs. 6 and 7) and the experimental data are presented in Fig. 10.

$$\frac{j^2}{j_m^2} = \frac{1.9542}{\frac{t}{t_m}}\left\{1 - \exp\left[-1.2564\,\frac{t}{t_m}\right]\right\}^2 \quad [6]$$

$$\frac{j^2}{j_m^2} = \frac{1.2254}{\frac{t}{t_m}}\left\{1 - \exp\left[-2.3357\,\frac{t^2}{t_m^2}\right]\right\}^2 \quad [7]$$

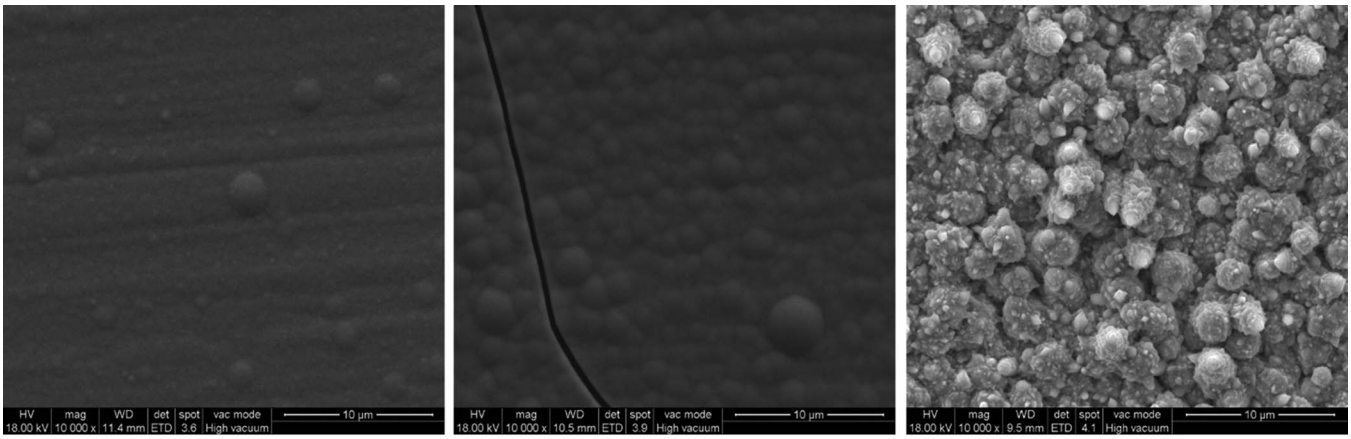

(a) (b) (c)

Figure 7. Scanning electron micrographs of galvanostatic copper deposits (a) 0.005 A cm^{-2} (b) 0.01 A cm^{-2} and (c) 0.02 A cm^{-2}.

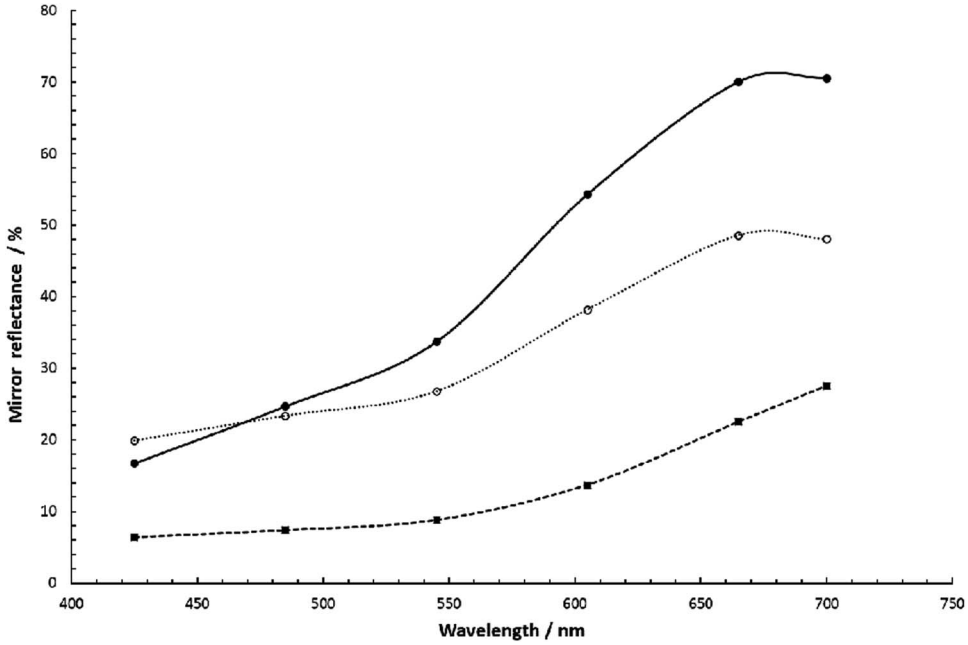

Figure 8. Mirror reflection of the galvanostatic copper deposits (—) 0.005 A cm^{-2}, (· · · ·) 0.01 A cm^{-2} and (- - -) 0.02 A cm^{-2} as a function of the wavelength.

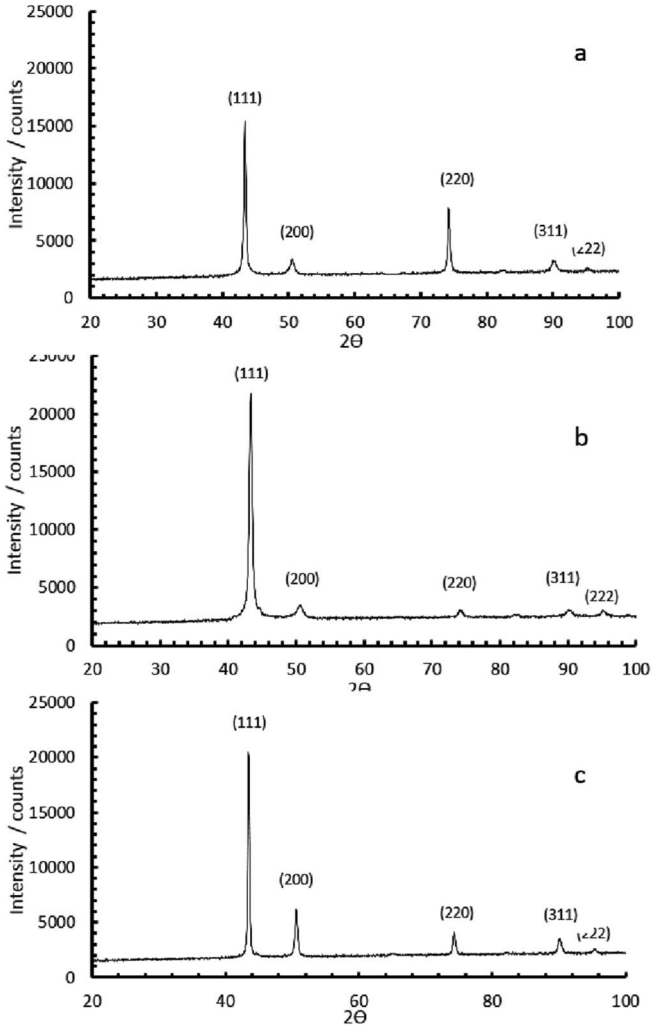

Figure 9. XRD patterns for the galvanostatic copper deposits (a) 0.005 A cm^{-2} (b) 0.01 A cm^{-2} and (c) 0.02 A cm^{-2}.

Table I. RTC values for the three copper deposits.

Peak (hkl)	RTC Bright sample (%)	RTC Semi-bright sample (%)	RTC Matte sample (%)
(111)	53	53	54
(200)	11	11	20
(220)	23	23	12
(311)	9	9	10
(222)	3	3	4

Experimental data compared with the two models indicates that nucleation takes place through a mechanism more similar to instantaneous nucleation. The deviation observed for (t/tm) > 1 can be attributed to the morphology of the nuclei, which are not spherical.[30] AFM images showing a large surface density of nuclei of quite uniform size confirmed this behavior. The sample corresponding to −0.60 V is shown in Fig. 11. For the three potentiostatic samples the same average surface density (10 nuclei/μm^2) of small (60–100 nm) copper crystals cover the entire surface. The arithmetic average of the roughness profile (Ra) as a function of the potential is presented in Fig. 12. It is clear that as the potential becomes more cathodic, Ra increases due to larger size of nuclei even though the nuclei density remains constant. This fact confirms that instantaneous nucleation is the basic process of the initial steps of coating formation, in which very small nuclei cover the entire surface at the very beginning. This could also account for the low roughness of the coating as a due to reduction of the extension of the exclusion zones between the nuclei. As a result, the electrolyte acts as a self-levelling plating bath.

Conclusions

A novel glutamate based electrolyte for copper electrodeposition on less noble substrates is presented. Its composition was adjusted in order to have only one soluble anionic cupric complex in the system. CV allowed the characterization of the electrochemical processes involved in copper deposition and dissolution for this electrolyte and the results suggest the existence of a cuprous intermediate in the reaction mechanism. In addition to this, potentiostatic studies helped identifying instantaneous nucleation of geometrical facetted nuclei as the copper nucleation mechanism on steel substrates for this electrolyte.

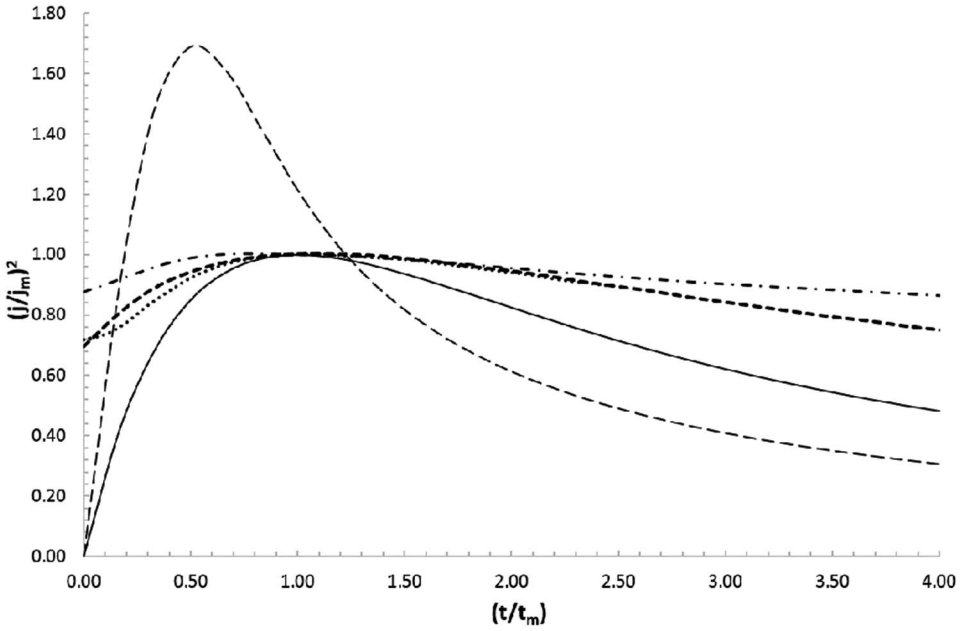

Figure 10. Nucleation models, instantaneous (—) and progressive (– – –), and experimental data collected from the chronoamperometric experiments at −0.50 (· · · ·), −0.60 (- - -) and −0.75 (- ● -) V/SCE.

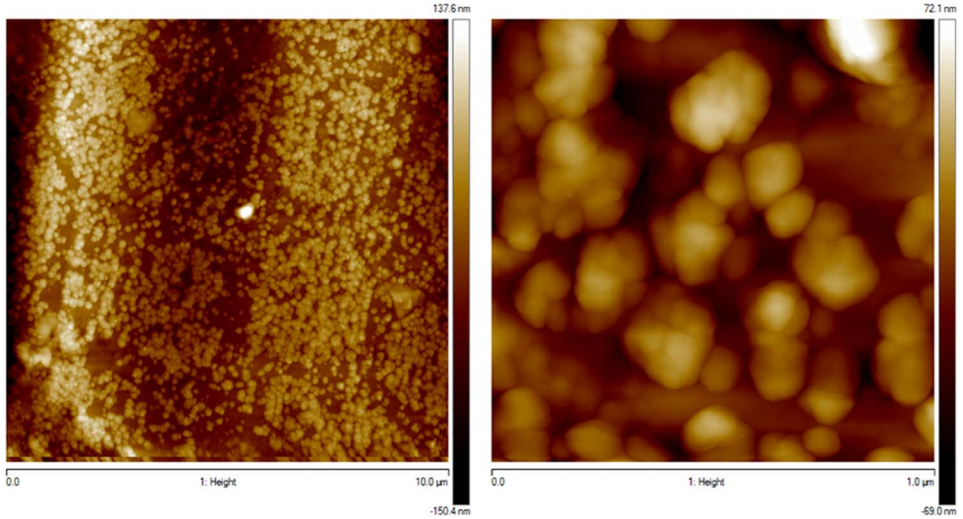

Figure 11. AFM images of the potentiostatic copper deposit obtained at −0.70 V/SCE.

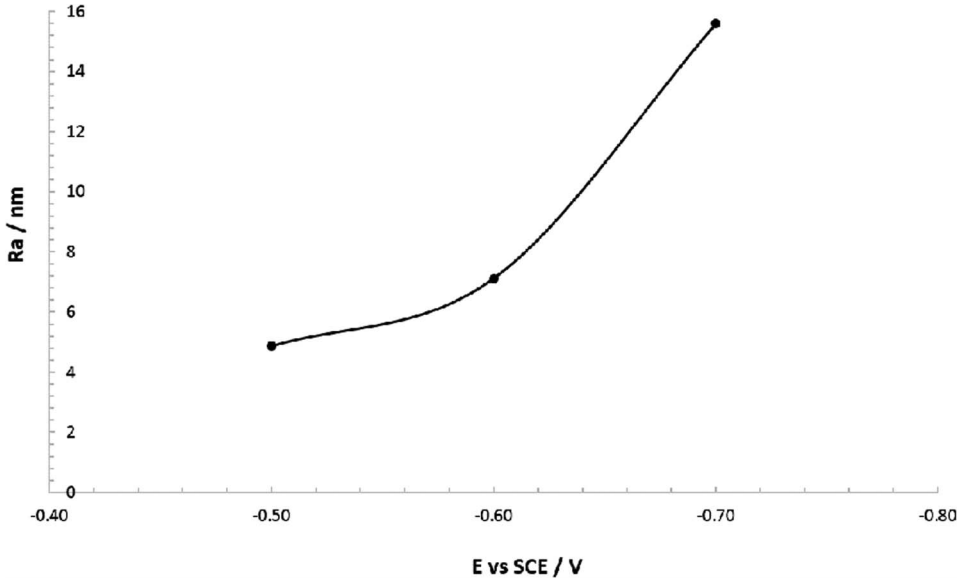

Figure 12. Arithmetic average roughness (Ra) as a function of the potential measure from a 1 μm^2 image.

Finally, galvanostatic experiments were able to produce thick deposits, which presented good quality characteristics at different CDs. All this evidence suggests that this copper-glutamate electrolyte is a good candidate for the replacement of cyanide in copper strike plating baths, and has a potential as a new bath capable of doing the complete copper plating in one step.

Acknowledgments

The authors thank the Comisión de Investigaciones Científicas de la Provincia de Buenos Aires (CICPBA), Consejo Nacional de Investigaciones Científicas y Técnicas (CONICET) and Universidad Nacional de La Plata (UNLP) for their financial support to this research and Eng. H. A. Lazzarino for the mirror reflectance measurements.

References

1. N. Piccinini, G. N. Ruggiero, G. Baldi, and A. Robotto, *J. Hazard. Mater.*, **71**, 395 (2000).
2. R. J. Barnhurst, in *ASM Handbook*, A. International Editor (1994).
3. J. K. Dennis and T. E. Such, *Nickel and chromium plating*, Woodhead Publishing Limited, Cambridge, England (1993).
4. C. V. Pecequilo and Z. Panossian, *Electrochimica Acta*, **55**, 3870 (2010).
5. A. Survila and V. Uksiené, *Electrochimica Acta*, **37**, 745 (1992).
6. Z. A. Hamid and A. A. Aal, *Surface and Coatings Technology*, **203**, 1360 (2009).
7. S. S. Abd El Rehim, S. M. Sayyah, and M. M. El Deeb, *Applied Surface Science*, **165**, 249 (2000).
8. S. Daniele and M. J. Pena, *Electrochimica Acta*, **38**, 165 (1993).
9. J. C. Ballesteros, E. Chaînet, P. Ozil, G. Trejo, and Y. Meas, *Journal of Electroanalytical Chemistry*, **645**, 94 (2010).
10. L. C. Tomaszewski and T. W. Tomaszewski, U.S. Pat. 4,469,569 (1984).
11. R. Stravitsky and B. D. Lovelock, U.S. Pat. 4,904,354 (1990).
12. J. A. Kline, U.S. Pat. 4,933,051 (1990).
13. E. Rohbani, U.S. Pat. 5,607,570 (1997).
14. R. M. Smith and A. E. Martell, *Critical stability constants. Volumen 6-Second Supplement*, Plenum Press (1989).
15. S. Adamek and C. A. Winkler, *Canadian Journal of Chemistry*, **32**, 931 (1954).
16. S. Royal Institute of Technology, MEDUSA (Make Equilibrium Diagrams Using Sophisticated Algorithms) Program http://www.ke-mi.kth.se/medusa in, Sweden.
17. M. Pourbaix, *Atlas of Electrochemical Equilibria in Aqueous Solutions*, p. 644, National Association of Corrosion Engineers, Houston, Texas, USA (1974).
18. J. Newman, *Journal of the Electrochemical Society*, **113**, 501 (1966).
19. E. Bottari, M. R. Festa, and R. Jasionowska, *Polyhedron*, **8**, 1019 (1989).
20. Y.-C. Liang and Å. Olin, *Acta chemica Scandinavica. Series A. Physical and inorganic chemistry*, **38**, 247 (1984).
21. N. C. Li and E. Doody, *J. Amer. Chem. Soc.*, **74**, 4184 (1952).
22. D. Grujicic and B. Pesic, *Electrochimica Acta*, **50**, 4426 (2005).
23. A. E. Bolzán, *Electrochimica Acta*, **113**, 706 (2013).
24. V. Kublanovsky and K. Litovchenko, *Journal of Electroanalytical Chemistry*, **495**, 10 (2000).
25. A. I. Danilov, E. B. Molodkina, and Y. M. Polukarov, *Russian Journal of Electrochemistry*, **36**, 987 (2000).
26. A. Survila and P. V. Stasiukaitis, *Electrochimica Acta*, **42**, 1113 (1997).
27. A. J. Bard and L. R. Faulkner, *Electrochemical methods. Fundamental and applications*, John Wiley & Sons, Inc., New York (2001).
28. R. S. Nicholson, *Anal. Chem.*, **37**, 1351 (1965).
29. E. Mattsson and J. O. M. Bockris, *Transactions of the Faraday Society*, **55**, 1586 (1959).
30. D. Grujicic and B. Pesic, *Electrochimica Acta*, **47**, 2901 (2002).
31. R. M. Smith and A. E. Martell, *Stability Constants. Volumen 2-Amines*, Plenum Press (1975).
32. M. B. Quiroga Argañaraz, C. I. Vázquez, and G. I. Lacconi, *Journal of Electroanalytical Chemistry*, **639**, 95 (2010).
33. R. Drissi-Daoudi, A. Irhzo, and A. Darchen, *Journal of Applied Electrochemistry*, **33**, 339 (2003).
34. J. Crousier and I. Bimaghra, *Electrochimica Acta*, **34**, 1205 (1989).
35. A. I. Danilov, E. B. Molodkina, and Y. M. Polukarov, *Russian Journal of Electrochemistry*, **38**, 732 (2002).
36. L. M. Abrantes, L. M. Castillo, C. Norman, and L. M. Peter, *Journal of Electroanalytical Chemistry and Interfacial Electrochemistry*, **163**, 209 (1984).
37. K. I. Popov and N. D. Nikolic, in *Electrochemical production of metal powders*, S. S. Djokic Editor, Springer, New York (2012).
38. N. D. Nikolić, G. Novaković, Z. Rakočević, D. R. Đurović, and K. I. Popov, *Surface and Coatings Technology*, **161**, 188 (2002).
39. N. D. Nikolić, Z. Rakočević, and K. I. Popov, *Journal of Electroanalytical Chemistry*, **514**, 56 (2001).
40. B. Scharifker and G. Hills, *Electrochimica Acta*, **28**, 879 (1983).